

Modeling, Simulation and Fault Diagnosis of a Doubly Fed Induction Generator using Bond Graph

A.T. BOUM*^A D.G.TATCHOU DJESSEU^B

^{ab} University of Buea,
ENSET-Kumba
PO.Box 63 Buea,
CAMEROON

*boumat2002@yahoo.fr

Abstract: Monitoring systems have a major role in the security of industrial plants and their equipments. Reporting to the operator as soon as possible the changes in behavior of the system in relation to the expected nominal behavior is primordial for the implementation of preventive and corrective actions on the process. This article deals with the modeling and diagnosis of the Double Fed Induction Generator (DFIG) defects based on the Bond Graph tool. Since the DFIG is mostly used in the electromechanical chains of conversion of wind turbines, or as engine and its operation is governed by several physical phenomena and various technological components. The Bond Graph tool is well adapted because it is based on an energy and multiphysical analysis. We introduce the modeling tool used and come out with a bond graph model of the DFIG. Diagnostic methods based on the Bond Graph model are applied for the faults detection and isolation in the DFIG. The results showed a good possibility of fault detection and therefore a possibility to use this approach for monitoring purpose.

Keywords: Defect, Diagnosis, Analytical Redundancy Relations, fault detection and isolation, DFIG

1. Introduction

The double fed induction machine (DFIM) is very popular because it has some advantages over all other variable speed types (such as cage asynchronous machine, or a synchronous generator.) It's used in the chain of electromechanical conversion of wind turbine or as engine and has experienced a spectacular growth in the last years [2], [22], [4]. In generator operation, it is best suited for the generation of constant frequency energy with variable speed drive. One of the advantages of dual power supply is that the rotor circuit can be controlled by a power converter. Indeed, the energy converter used to rectify and undulate the alternating currents of the rotor has a nominal power fractional to that of the stator, which makes it possible to achieve better control of the power transfers with significantly improved efficiency and reduces its cost Compared to competing topologies [8].

Systems designed and manufactured by man (vehicles, aircraft, telecommunications networks, factories, etc. . . .) are becoming increasingly complex. This complexity is due to the large number of components making up these systems. Despite the need for high security, reduced operating costs and control of equipment availability, these systems are not immune to failures. Therefore, monitoring, diagnosis (detection, localization, identification of failures), repair or reconfiguration are very important [31]. These activities can detect and locate defaults, minimize repair time, and provide a reliable and easily interpretable diagnosis despite the complexity of the equipment [25], [35],

[14]. The diagnosis of the systems appeared in order to ensure the detection, localization, and identification of failures and it became a topic of strategic importance.

In this work, modeling, simulation and fault diagnosis of the DFIG is addressed [5], [11]. This paper is organized as follows, Section 2 is related to the modeling and simulation, Section 3 deals to the diagnosis of DFIG, with the discussions of the simulation results. Finally, the conclusions of the paper are presented in Section 4.

2. Bond Graph modeling and simulation

Unlike the asynchronous machine, the double fed induction machine is a wound rotor machine for which rotor windings are fed. Figure below shows a scheme of a double fed induction machine with symmetrical 3-phase winding in both stator and rotor.

Modeling assumptions are:

Magnetic isotropy (due to material isotropy and round rotor geometry, uniform air gap) in both stator and rotor is assumed as well as magnetic linearity, we work in an unsaturated regime, Eddy current losses and hysteresis phenomena are neglected, homopolar is vanished because the neutral is not connected, symmetrical stator (subscript s for its parameters and variables) with sinusoidally distributed, symmetrical rotor (subscript r for its parameters and variables) with sinusoidally distributed, Y-connected windings.

For easier modeling of the doubly fed induction generator, the dq reference frame is chosen. Furthermore, as generator convention is considered, which means that the currents are

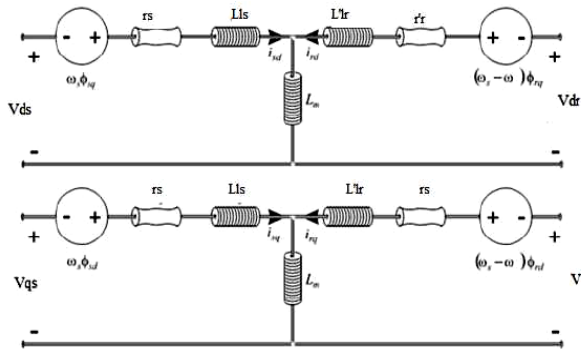


Figure 1: equivalent circuit of the DFIG in dq reference frame

outputs instead of inputs: thus, $i_s \rightarrow -i_s$ and $i_r \rightarrow -i_r$. Active and reactive power have a positive sign when they are fed into the grid [28]. Using the generator convention, one have the following set of stator and rotor equations in the dq reference frame linked to the rotating field.

$$V_{ds} = -r_s i_{ds} - \omega_s \varphi_{qs} + d(\varphi_{ds})/dt \tag{1}$$

$$V_{qs} = -r_s i_{qs} + \omega_s \varphi_{ds} + d(\varphi_{qs})/dt \tag{2}$$

$$V_{dr} = -r_r i_{dr} - (\omega_s - \omega) \varphi_{qr} + d(\varphi_{dr})/dt \tag{3}$$

$$V_{qr} = -r_r i_{qr} - (\omega_s - \omega) \varphi_{dr} + d(\varphi_{qr})/dt \tag{4}$$

$$\omega_r = \omega_s - \omega \tag{5}$$

and the flux linkages becomes:

$$\varphi_{ds} = -L_s i_{ds} - M i_{dr} \tag{6}$$

$$\varphi_{qs} = -L_s i_{qs} - M i_{qr} \tag{7}$$

$$\varphi_{dr} = -L_r i_{dr} - M i_{ds} \tag{8}$$

$$\varphi_{qr} = -L_r i_{qr} - M i_{qs} \tag{9}$$

Active and reactive power to the stator and the rotor are calculated as follow:

$$P_s = v_{ds} i_{ds} + v_{qs} i_{qs} \tag{10}$$

$$P_r = v_{dr} i_{dr} + v_{qr} i_{qr} \tag{11}$$

$$Q_s = v_{qs} i_{ds} - v_{ds} i_{qs} \tag{12}$$

$$Q_r = v_{qr} i_{dr} - v_{dr} i_{qr} \tag{13}$$

and the net active and reactive power injected into the grid is computed as follow:

$$P = P_s + P_r \tag{14}$$

$$Q = Q_s + Q_r \tag{15}$$

Figure 2: Electromagnetic torque, mechanical torque in DFIG and angular speed of the rotor

2.1. Modeling and simulation

To model the DFIG we have two inputs: the angular speed Ω and the rotor voltages (V_{qr} and V_{dr}) and the output (P and Q) are calculated through the model.

2.1.1. Parameters of the machine used for simulation

The studied machine is a 2 poles pairs Leroy-Somer wounded-rotor induction machine. Its parameters are given below [16]

Electrical:

Stator per phase resistance: $R_s = 0,455\Omega$

Rotor per phase resistance: $R'_r = 0,62\Omega$

Stator leakage Inductance: $L_{ls} = 0,006H$

Rotor leakage inductance: $L'_{lr} = 0,003H$

Magnetizing inductance: $M = 0,078H$.

Mechanical:

Inertia: $J = 0,3125kg.m^2$.

Viscous friction $b = 6,73.10^{-3}N.m.s^{-1}$.

The voltage injected into the rotor and stator windings with frequencies are:

Rotor voltage and frequency: $V_r = 22V_{rms}, f_r = 10hertz$

Stator voltage and frequency: $V_s = 220V_{rms}, f_s = 50h$

To emulate variable speed, we will variate the angular speed from $\Omega = 125,6rad/s$ to $\Omega = 160rad/s$ at $t = 1s$ and from $\Omega = 160rad/s$ to $\Omega = 188,4rad/s$ at $t = 2s$. One has the figures below.

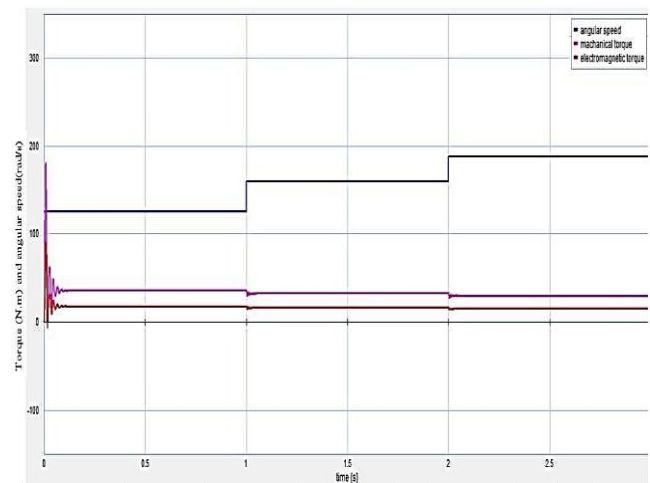


Figure 2 shows the angular speed, the mechanical and electromagnetic torques of the machine. They stabilizes rapidly (**0.1s**) by operating in supersynchronous mode. The mechanical torque is **29.89N.m** and the electromagnetic one is **14.94N.m**. These values decrease according to the variation of the speed. Concerning the power generated by the machine, the activ power to the stator, to the rotor and the net injected are stabilized also after **0.1s** and reached at start up values of

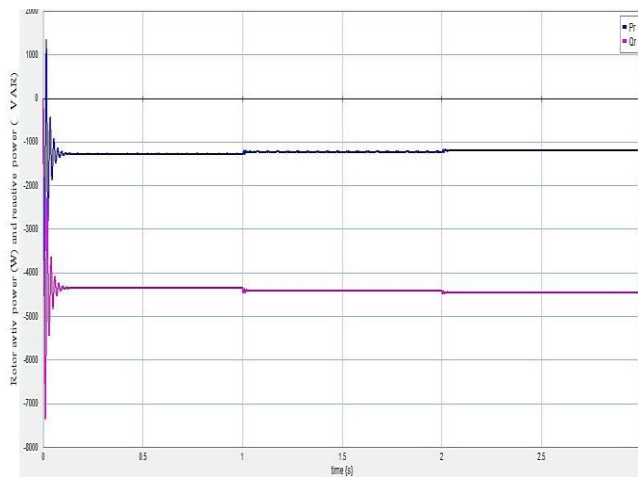


Figure 3: Rotor active and reactive power

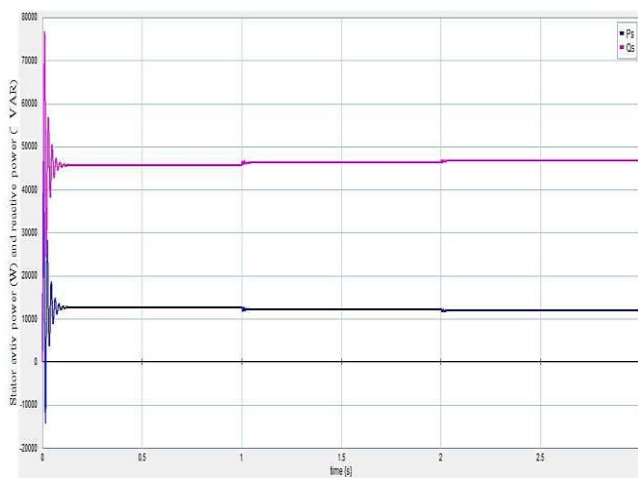


Figure 4: Stator active and reactive power

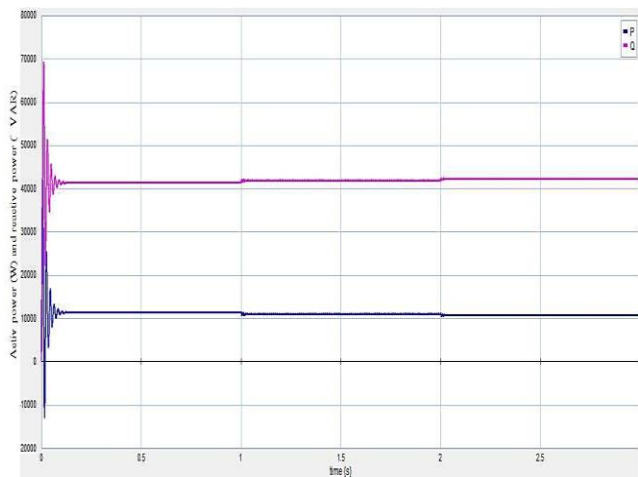


Figure 5: Net active and reactive power injected into the grid

the order of two to three times the rated power in steady state. The power generated varies with the angular speed.

3. Bond Graph Diagnosis of the DFIG

In order to ensure the safe operation of the systems, Fault Detection and Isolation (FDI) techniques have been implemented. Fault Detection and Isolation through Bond Graph uses the notion of Analytical Redundancy Relations to quickly detect the operation of the machine in a mode different from the normal one. In this section, we will apply the ARR's generation algorithm detailed in [17], [43] for the fault diagnosis of the DFIG [2], [11].

The BG model of the DFIG dedicated for the diagnosis is given in the figure 6: we note that, as said in [19], to represent real system elements or components explicitly, certain bond graph elements should be moved, altered, or added. This is the reason why the resistances in the diphasic reference frame has been moved and split into three stator and three rotor coil resistances R_{s1}, R_{s2}, R_{s3} and R_{r1}, R_{r2}, R_{r3} , to make explicit the resistance of each of the stator and rotor coils.

3.1. ARR's generation algorithm

The algorithm for generating ARR's from the BG model for diagnosis is summarily carried out according to the following steps [17],[43], [11]:

1. Put the Bond Graph model in differential preferred causality BGD (by reversing causality of the detectors if possible).
2. Identify the structure junctions "0" and "1" containing at least one detector. Write the equations of the obtained model; equations of the junctions, sources and control.
3. For any detector whose causality is reversed an ARR is deduced,

$$\sum b_i f_i + \sum S f_i \quad ; \quad \text{for a 0-junction.}$$

$$\sum b_i e_i + \sum S e_i \quad ; \quad \text{for a 1-junction.}$$

$b_i = \pm 1$ depending on whether the half-arrow goes in or out of the junction. The unknown variables, effort (e) and flux (f) are then eliminated by going through the causal path from the known variable ($SSf: f_m$ et $SSe: e_m$) to the unknown one. The ARR coming from the junction "0" will have as unit the one of the flux and the one coming from the junction "1" the effort. Each of the ARR's will be sensitive to faults that may affect the component traversed by the causal path for the elimination of unknown variables.

4. For any detector whose causality cannot be reversed, an ARR is deduced by putting its output in equality with the output of another detector of the same type (hardware redundancy).

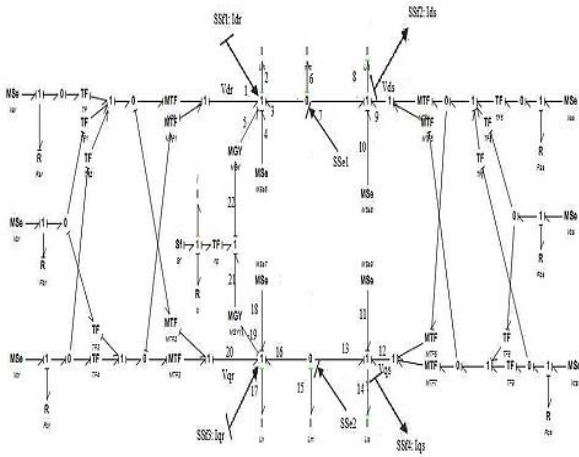


Figure 6: Bond Graph of the DFIG used for the diagnosis

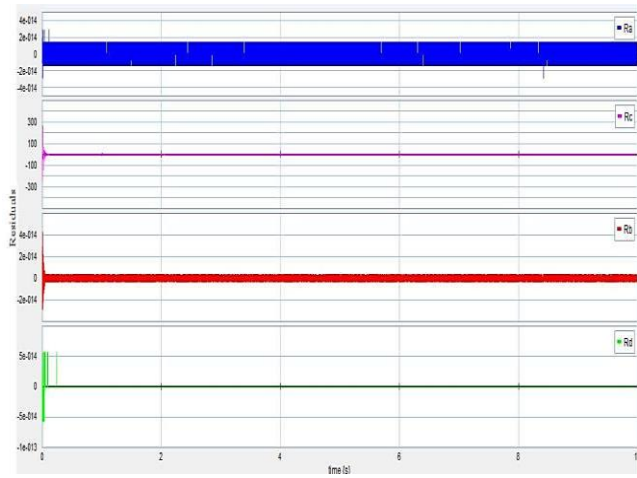


Figure 7: Residuals R_a , R_b , R_c , and R_d of the DFIG in healthy condition (for variable speed)

Figure 6 shows the Bond Graph model of the DFIG in differential preferred causality for the diagnosis.

Let's call the 1-junctions with SSF_1 , SSF_2 , SSF_3 and SSF_4 junctions a, b, c, and d respectively.

Equations for the junctions a, b, c and d are

$$(a) : e_1 - e_2 + e_3 + e_4 + e_5 = 0 \quad (16)$$

$$(b) : e_9 - e_8 + e_{10} + e_7 = 0 \quad (17)$$

$$(c) : e_{20} - e_{19} + e_{18} + e_{16} - e_{17} = 0 \quad (18)$$

$$(d) : e_{11} + e_{12} + e_{13} - e_{14} = 0 \quad (19)$$

Therefore, we have the residuals that follow:

$$R_a : V_{dr} - \frac{d(SSf_1)}{dt} + \omega_s \varphi_{qr} + SSf_1 + 2S_f * r_{GY} \quad (20)$$

$R_b : V_{qs} - \frac{d(SSf_2)}{dt} + \omega_s \varphi_{qs} + SSf_2$
 The generator is still operating in variable speed. The angular speed move from $\Omega = 125.6 \text{ rad/s}$ to $\Omega = 160 \text{ rad/s}$ at $t = 1.5 \text{ s}$ and from $\Omega = 160 \text{ rad/s}$ to $\Omega = 188.4 \text{ rad/s}$ at $t = 2 \text{ s}$. The residuals of the DFIG operating in healthy conditions are shown in figure 7.

A phase to phase short circuit to the stator (at $t = 1.5 \text{ s}$) of the DFIG produce residuals in figure 10.

A single phase operation in the stator of the DFIG at $t = 1.5 \text{ s}$ gives the residuals in figure 15.

A phase to phase short circuit to the rotor (at $t = 1.5 \text{ s}$) of the DFIG produces the residuals in figure 16.

A rotor rolling break (at $t = 1.5 \text{ s}$) of the DFIG gives the residuals in figure 17.

A short circuit between two phases of the stator and the rotor shows that at the moment of the faults, the currents in the stator

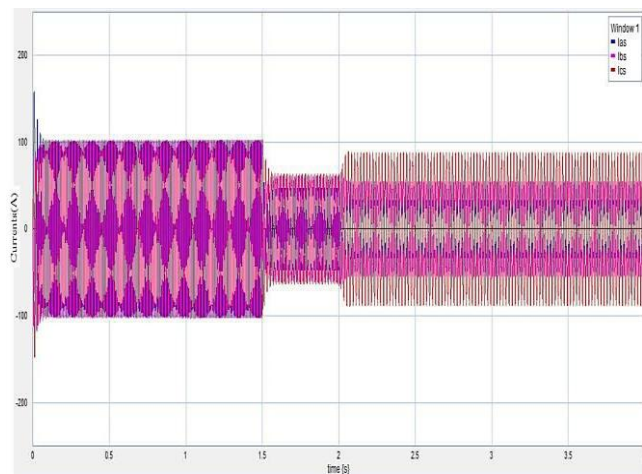


Figure 8: Currents i_{as} , i_{bs} , i_{cs} with a phase to phase short circuit in the stator at $t = 1.5 \text{ s}$ (For variable speed)

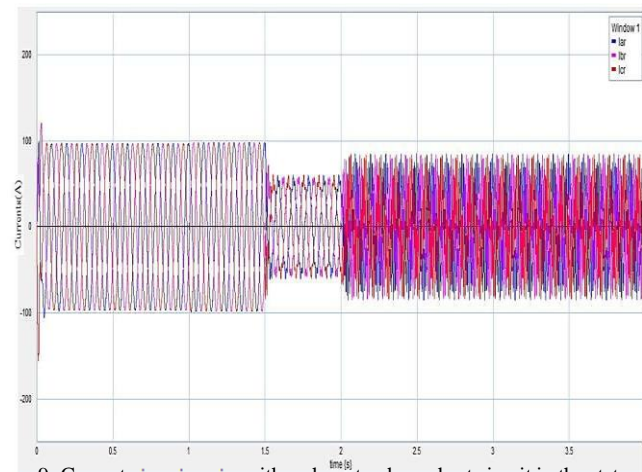


Figure 9: Currents i_{ar} , i_{br} , i_{cr} with a phase to phase short circuit in the stator at $t = 1.5 \text{ s}$ (For variable speed)

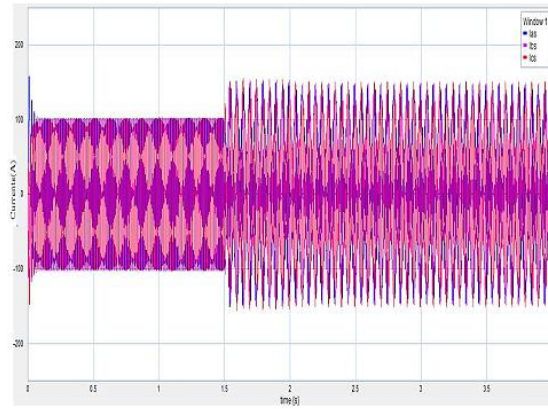
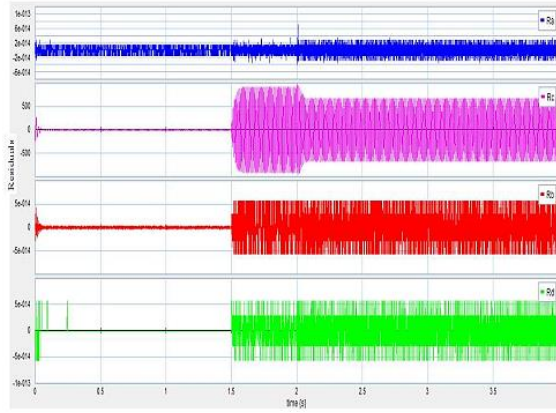


Figure 10: Residuals R_a , R_r , R_b and R_d of the DFIG with a phase to phase short circuit in the stator at $t = 1.5s$ (for variable speed)

Figure 13: Currents i_a , i_b , i_c with a short circuit in rotor winding at $t = 1.5s$ (For variable speed)

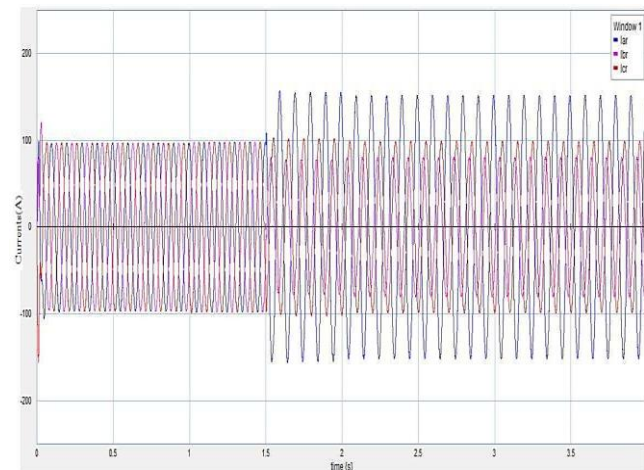
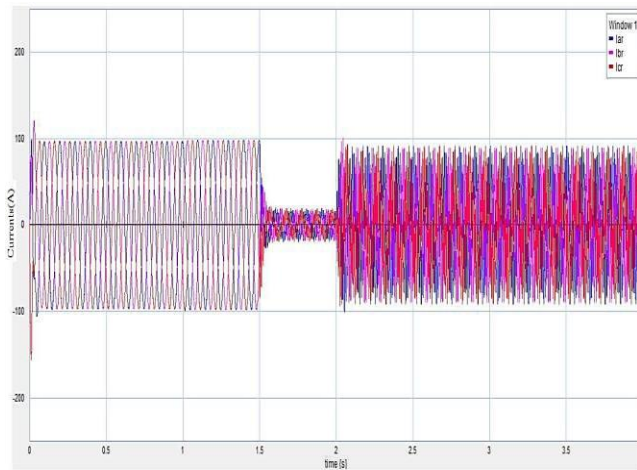


Figure 11: Currents i_a , i_b , i_c with an open phase in stator winding at $t = 1.5s$ (for variable speed)

Figure 14: Currents i_a , i_b , i_c with a short circuit in rotor winding at $t = 1.5s$ (For variable speed)

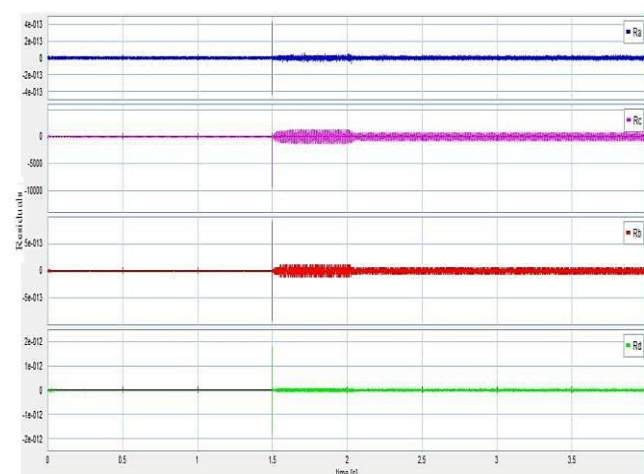
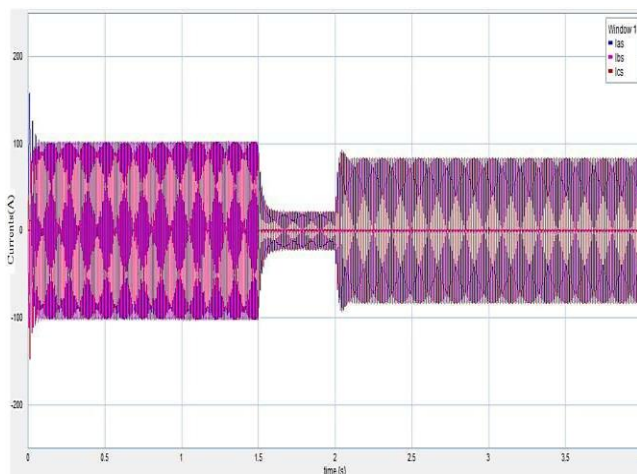


Figure 12: Currents i_a , i_b , i_c with an open phase in stator winding at $t = 1.5s$ (For variable speed)

Figure 15: Residuals R_a , R_r , R_b and R_d of the DFIG with an open phase in the stator at $t = 1.5s$ (for variable speed)

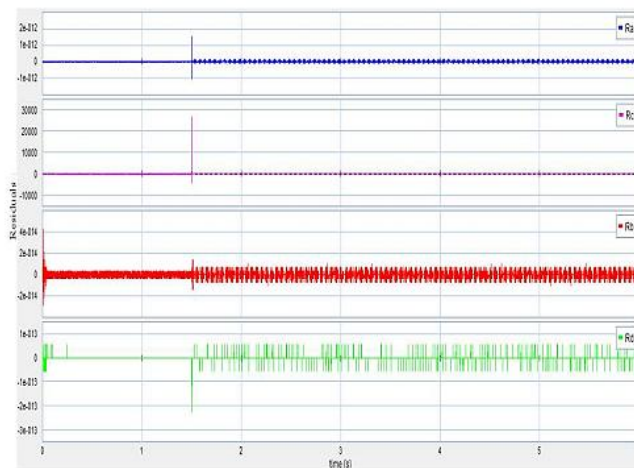


Figure 16: Residuals R_a , R_b , R_c , and R_d of the DFIG with phase to phase short circuit in the rotor at $t = 1.5s$ (for variable speed)

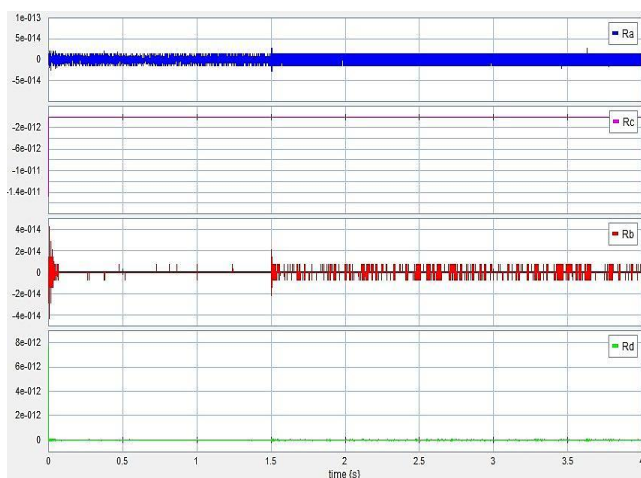


Figure 17: Residuals R_a , R_b , R_c , and R_d of the DFIG with a rotor rolling break at $t = 1.5s$ (for variable speed)

windings become unbalanced. In addition, it should also be noted that this short circuit also has an effect on the currents of the rotor windings which see their amplitudes decrease and their shapes change from the time of the occurrence of the defect.

During an open phase stator, the current in the open phase is nearby zero and it is found that the machine is powered by a two phase. And in the same way as before, the rotor current system is no longer the same in amplitude and shape as soon as the defect occur rotor rolling break defect.

The results obtained show that for stator faults (short circuit between phase and phase break for fixed and variable speed), all the residual curves obtained from the ARR have their amplitude and shape modified. While for a fault at the rotor, one of the residues at least is not altered whatever the defect.

A fault on the DFIG is detected by the modification of the residuals amplitude or shape from the moment of occurrence of the defect (only the rotor defects leave at least one residual almost insensitive). The isolation is obtained by the total sensitivity (for a stator defect) or partial (for a rotor defect) of the ARR.

4. Conclusion

In the current energy context, the performance of energy production systems is increasing. They must always produce better, at lower cost and under conditions of security not always reliable. In addition, the processes are increasingly complex and increasingly computerized. Thus, it is less and less obvious or intuitive to know if everything is going well in a process. To this end, monitoring of processes allows the detection and diagnosis of anomalies (of faults). Thus, the more quickly a fault is detected and correctly diagnosed, the more the production will not be interpreted and will meet the requirements. We presented an interesting diagnostic method by Bond Graph that allows to include in a same tool: modeling and diagnosis.

The use of the Bond Graph tool for modeling and the detection of defects in DFIG has appeared to be very efficient because of its simplicity and its adaptation for different multi-physical systems (electrical engineering, mechanical engineering, hydraulic...). Our contribution concerns the application of a method based on the Bond Graph to model, and then generate Analytical Redundancy Relations (residuals) for the detection and isolation of defects.

Nomenclature

L'_{ls} and L'_{lr} are stator and rotor leakage inductances referred to the stator side.

r'_s and r'_r are stator and rotor resistance referred to the stator.

L_m is the magnetising inductance.

n_p is the number of pole pairs.

Ω is the angular velocity of the rotor

v_{ds} and v_{qs} are the stator voltages in the dq frame.

v_{dr} and v_{qr} are the rotor voltages in the dq frame.

i_{ds} and i_{qs} are the stator currents in the dq frame.

i_{dr} and i_{qr} are the rotor currents in the dq frame.

θ_s and θ_r are angles of Park's transformation respectively for stator and rotor parameters.

φ_{dqr} are stator and rotor fluxes in the dq frame

φ_{dqqs} are stator and rotor fluxes in the dq frame

P_s and Q_s are stator active and reactive power

P_r and Q_r are rotor active and reactive power

ω_s is the electrical rotating speed of the stator flux

ω_r is the electrical rotating speed of the rotor flux

M is the mutual inductance

5. References

- [1] S. KAYAL A. KUMAR, B. MUNSHI. Study of wind turbine driven dfig using ac/dc/ac converter. Technical report, National Institute of Technology, Rourkela-769008, 2009.
- [2] Belkacem Ould Bouamama Seddik Bacha Abd Essalam Badoud, Mabrouk Khemliche. Bond graph algorithms for fault detection and isolation in wind energy conversion. Arabian Journal for Science & Engineering (Springer Science & Business Media, 39(5):4057–4076, 2014.

- [3] Boukaroura Abdelkader. Modélisation et diagnostic d'un onduleur triphase par l'approche bond graph. Master's thesis, UNIVERSITE FERHAT ABBAS DE SETIF, 2009.
- [4] Barazane Linda Abdelmalek Samir and Abdelkader Larabi Houari Boumediene. Diagnosis of short-circuit faults (scf) in the doubly fed induction generator (dfig). *Journal of Automation & Systems Engineering*, 10(4):196–203, 2016.
- [5] Lachouri Abderrazak, Ramdane Adlene, and Krikeb Mohamed. Modeling and simulation of a wind turbine driven induction generator using bond graph. *Renewable Energy and Sustainable Development*, 2(1):236–242, 2015.
- [6] MELLOUL Ahmed. Simulation et diagnostic d'une machine asynchrone à double alimentation d'une éolienne. Master's thesis, UNIVERSITE FERHAT ABBAS, 2011.
- [7] L. Baghili. Modélisation et Commande de la Machine Asynchrone. 2004.
- [8] Hakim Bennani. MACHINE ASYNCHRONE A DOUBLE ALIMENTATION Les lois de commande en régime permanent. PhD thesis, UNIVERSITÉ LAVAL QUÉBEC, 2015.
- [9] Wolfgang Borutzky. *Bond Graph Methodology. Development and Analysis of Multi-disciplinary Dynamic System Models*. Springer, 2010.
- [10] Wolfgang Borutzky. *Bond Graph Modelling of Engineering Systems, Theory, Applications and Software Support*. Springer, 2011.
- [11] Wolfgang Borutzky. *Bond Graphs for Modelling, Control and Fault Diagnosis of Engineering Systems*. Springer, 2017.
- [12] E. Fossas C. Batlle, A. Dòria-Cerezo. Hybrid model of a doubly-fed induction machine and a back-to-back converter. Technical report, Institut d'organisasi i control des systemes industriels, 2005.
- [13] G. Dauphin-Tanguy and al. *Les Bond Graphs pour : la modélisation, la commande et la surveillance*. 2011.
- [14] Abdelkader Mami Dhia Mzoughi, Abderrahmene Sallami. The performance of the bond graph approach for diagnosing electrical systems. *International Journal of Advanced Computer Science and Applications*, 8(7):76–81, 2017.
- [15] W. Elost. *Surveillance structurelle et platitude pour le diagnostic des modèles Bond Graph couplés*. PhD thesis, Université des sciences et technologie de Lille, France, 2005.
- [16] T. Bouaouiche F. Poitiers and M. Machmoum. Advanced control of a doubly-fed induction generator for wind energy conversion. Article in *Electric Power Systems Research*, 2009.
- [17] Z. Simeu Abasi M. Hassani H.Dhouibi, M.Bochra. Diagnosis approach using bond graph and timed automata. *International Journal of Advanced Research in Electrical, Electronics and Instrumentation Engineering*, 2, sep 2013.
- [18] Ali IBRAHIM. Contribution au diagnostic de machines électromécaniques. PhD thesis, ÉCOLE DOCTORALE SCIENCES, INGÉNIERIE, SANTÉ, 2009.
- [19] Michael D. Bryant Jongbaeg Kim. Bond graph model of a squirrel cage induction motor with direct physical correspondence. *Journal of Dynamic Systems, Measurement, and Control*, 122, 2000.
- [20] S.Paramasivam. K.Mohanraj, Sridhar Makkapati. Unbalanced and double line to ground fault detection of three phase vsi fed induction motor drive using fuzzy logic approach. *International Journal of Computer Applications*, 47(15), jun 2012.
- [21] W. Lee and al. Fault detection in an air hand-ling unit using residual and recursive parameter identification methods, pages 528–539. 1996.
- [22] Mijatovic N. Holbøll J. Skrimpas G. A. & Sweeney C. W Martens, S. Simulation of electric faults in doubly-fed induction generators employing advanced mathematical modelling. 2015.
- [23] Mohsen Montazeri Mohammad Ghasem Kazemi. A new robust fault diagnosis approach based on bond graph method. *The Brazilian Society of Mechanical Sciences and Engineering*, 39:4353–4365, 2017.
- [24] Surya Santoso Mohit Singh. Dynamic models for wind turbines and wind power plants. Technical report, National Renewable Energy Laboratory, The University of Texas at Austin, 2011.
- [25] A. Mojallal and S. Lotfifard. Dfig wind generators fault diagnosis considering parameter and measurement uncertainties. *IEEE Transactions on Sustainable Energy*, 99:1–1, 2017.
- [26] BOUTASSETA Nadir. Diagnostic robuste des systemes energetiques par l'approche bond graph. Master's thesis, UNIVERSITE BADJIMOKHTAR ANNABA, 2014.
- [27] W. Nuninger. Stratégie de diagnostic robuste à l'aide de la redondance analytique. PhD thesis, Thèse de Doctorat université de Lorraine, 1997.
- [28] Constantin Bulac Oana Mănicuta, Mircea Eremia. dynamic simulation of double fed induction wind generators in the romanian power system. *U.P.B. Sci. Bull*, 77, 2015.
- [29] H. M. Paynter. *Analysis and design of engineering systems*. MIT Press, 1961.
- [30] Héctor Pulgar-Painemal. *Basics of DFIG power generation*. Universidad Técnica Federico Santa Maria Valparaiso, may 2013.
- [31] ABDELKADER LARABI SAMIR ABDELMALEK, LINDA BARAZANE. Fault diagnosis for a doubly fed induction generator. *Rev. Roum. Sci. Techn. Électrotechn. et Énerg.*, 61(2):159–163, 2016.
- [32] Farhad Shafiei. Modelling and verification of doubly fed induction generator (dfig) using real time digital simulator (rtds). Master's thesis, CHALMERS UNIVERSITY OF TECHNOLOGY, 2012.
- [33] M. Singh and al. Simulation for wind turbine generators with fast and matlab-simulink modules. Technical report, National Renewable Energy Laboratory, Department of Energy, Office of Energy Efficiency and Renewable Energy, 2014.
- [34] Michael A. Snyder. Development of simplified models of doubly-fed induction generators (dfig). a contribution towards standardized models for voltage and transient stability analysis. Master's thesis, Chalmers University of Technology, 2012.
- [35] Roberto Tapia and A Medina. Doubly-fed wind turbine generator control: A bond graph approach. *Simulation modelling practice and theory*, 53:149–166, 2015.
- [36] Hamid Reza Karimi Tore Bakka. Bond graph modeling and simulation of wind turbine systems. *Journal of Mechanical Science and Technology*, 27, 2013.
- [37] R. Toscano. *Commande et diagnostic des systèmes dynamiques*. Ellipses, Paris, 2005.
- [38] Youcef Touati. Diagnostic Robuste et estimation de Defauts a base de model Bond Graph. PhD thesis, Doctorat de l'universite Lille 1, 2012.
- [39] John Montgomery Vjekoslav Damic. *Mechatronics by bond graphs: an object-oriented approach to modeling and simulation*. Springer, 2003.
- [40] Stefan Wiechula. Tools for modelling and identification with bond graphs and genetic programming. Master's thesis, University of Waterloo, 2006.
- [41] Serge Scavarda Wilfrid Marquis-Favre. Alternative causality assignment procedures in bond graph for mechanical systems. *Journal of Dynamic Systems, Measurement, and Control*, 124, 2002.
- [42] Richard Zobel Wolfgang Borutzky, Alexandra Orsoni, editor. proceeding 20th European Conference on Modeling and Simulation, 2006.
- [43] B. OULD BOUAMAMA Y. TOUATI, R. MERZOUKI. Fault estimation and isolation using bond graph approach. 8th IFAC Symposium on Fault Detection, Supervision and Safety of Technical Processes (SAFE-PROCESS), 29(31), aug 2012.